



Passively Q-switched operation of in-band pumped Ho:YLF based on $Ti_3C_2T_x$ MXene

Cheng Zhang^a, Feng Zhang^b, Xiuwei Fan^a, Jimin Yang^a, Jie Liu^{a,*}, Han Zhang^b

^a Shandong Provincial Engineering and Technical Center of Light Manipulations & Shandong Provincial Key Laboratory of Optics and Photonic Device, School of Physics and Electronics, Shandong Normal University, Jinan 250358, China

^b SZU-NUS Collaborative Innovation Centre for Optoelectronic Science & Technology, and Key Laboratory of Optoelectronic Devices and Systems of the Ministry of Education and Guangdong Province, College of Optoelectronic Engineering, Shenzhen University, Shenzhen 518060, China

ARTICLE INFO

Keywords:

$Ti_3C_2T_x$ MXene
In-band pumped
passively Q-switched
Ho:YLF
2.1 μm

ABSTRACT

For the first time, the promising material, $Ti_3C_2T_x$ MXene, is successfully utilized as a saturable absorber to achieve a passively Q-switched operation of a 2.1 μm Ho:YLF laser. The maximum average output power of 341 mW is realized in the Tm: fiber in-band pumped Ho:YLF laser with the shortest pulse width of 837 ns corresponding to a single pulse energy and a peak power of 20.8 μJ and 7.43 W, respectively. The results prove that $Ti_3C_2T_x$ is an efficient optical modulator with the potential for important applications in the field of 2.1 μm ultrashort pulse lasers.

1. Introduction

Passively Q-switched solid-state lasers based on Ho^{3+} ions operating slightly over 2 μm have important applications in remote sensing, radar, medical, and pumping of optical parametric oscillators [1–4]. Ho lasers are generally in-band pumped into the 5I_7 energy level mainly by Tm-fiber or Tm-doped solid-state lasers around the wavelength range of ~ 1.9 – 1.95 μm . Compared with the Tm-doped solid-state lasers, commercial Tm: fiber sources can supply a mature manipulation with high power, beam quality, and optional emission wavelength (1.8–2 μm) [5]. Moreover, the in-band pumped Ho pulse laser has the characteristics of less heat and high efficiency because of its small quantum loss [6]. In effectuating the high-energy Q-switched mode, Ho-doped fluorides are more outstanding laser mediums than Ho:YAG because they own much longer upper laser-level lifetimes (~ 14 ms) and larger emission cross-sections (1.6×10^{-20} cm^2 around 2050 nm versus 1.2×10^{-20} cm^2 around 2090 nm of the Ho:YAG crystal), but smaller crystal splitting than Ho:YAG [7]. Continuous wave and actively Q-switched Ho:YLF lasers have been extensively researched upon; however, only a few papers have covered nanosecond pulse passively Q-switched (PQS) Ho:YLF lasers up to now [8–10].

PQS lasers based on saturable absorbers (SAs) are mostly accompanied by remarkable merits, for instance, connatural compactness,

simplicity, and low cost [11–18]. The two-dimensional (2D) material, MXene-SA, has recently brought new opportunities for PQS lasers because of its unique and distinct optical properties [19–23]. MXene is usually prepared by optionally etching out the A tiers from the $M_{n+1}AX_n$ phases, where M is the initial transition metal, and X is carbon and/or nitrogen [24]. The first successfully prepared and most studied 2D material is $Ti_3C_2T_x$, which has the advantages of good conductivity, tunable bandgap, and easy fabrication [25–30]. $Ti_3C_2T_x$ has a tier configuration (e.g., graphene, whose inter-tier length is 0.98 nm) [31]. The lower linear absorption of $Ti_3C_2T_x$ ($\sim 1\%$ /nm) produces a loss contrasting that of graphene (2.3% each atomic tier) [32–34]. Unlike other 2D materials, $Ti_3C_2T_x$ shows a higher threshold for light-induced damage, and the nonlinear transmittance is improved [35]. In addition, the zero-gap band texture of Ti_2C_3 (e.g., < 0.2 eV of $Ti_3C_2T_x$) has a broadband optical character of the wavelength from visible light to mid-infrared light [36–37]. As for the 2D materials, only graphene has ever been used as the SA in Ho:YLF lasers [9]. To the best of our knowledge, until now, no report has focused on the PQS performance based on $Ti_3C_2T_x$ of the Ho laser around 2.1 μm .

This study first demonstrates an integrated research on the PQS laser operations in a $Ti_3C_2T_x$ -based Ho:YLF laser pumped by a 1.94 μm fiber laser. A contrast analysis of the laser characteristics with two different output lenses is then performed. The maximum average output

* Corresponding author.

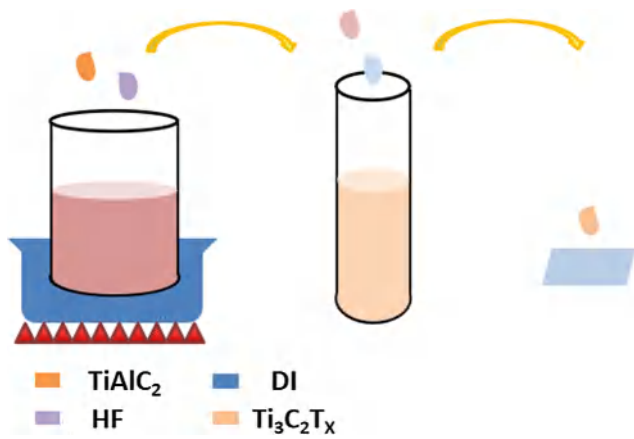
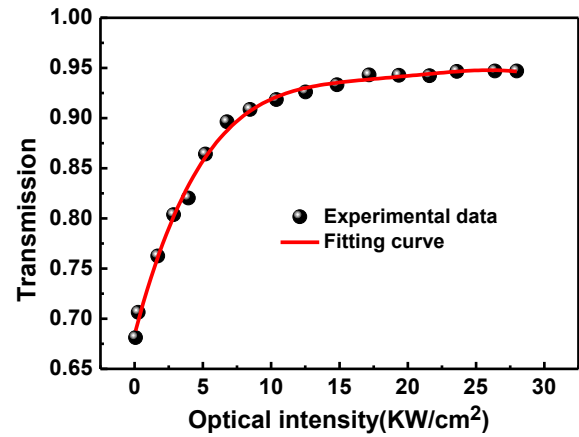
E-mail address: jieliu@sdsu.edu.cn (J. Liu).

<https://doi.org/10.1016/j.infrared.2019.103076>

Received 3 September 2019; Received in revised form 9 October 2019; Accepted 9 October 2019

Available online 10 October 2019

1350-4495/© 2019 Elsevier B.V. All rights reserved.

Fig. 1. Fabrication process of $\text{Ti}_3\text{C}_2\text{T}_x$.Fig. 3. Nonlinear absorption property of $\text{Ti}_3\text{C}_2\text{T}_x$.

power of 341 mW corresponding to the shortest pulse width of 837 ns and the repetition rate of 35.5 kHz is acquired in the PQS laser.

2. Fabrication and characteristics of $\text{Ti}_3\text{C}_2\text{T}_x$ -SA

The $\text{Ti}_3\text{C}_2\text{T}_x$ -SA used in our experiment was prepared through an acid etching process at room temperature (Fig. 1(a)). First, 2 ml Ti_3AlC_2 and 30 ml hydrofluoric acid (HF) were mixed in a beaker. The solution was then heated to 48 °C in a water bath pot and evenly stirred. After 6 h, 1 ml of the solution was dripped into the test tube and added with deionized water. The diluted solution was placed and centrifuged at 4000 rpm for 3 min, then the pH was measured. The earlier steps were repeated until the pH was maintained between 4 and 6. Finally, the supernatant was taken onto the quartz plate and dried at room temperature to obtain $\text{Ti}_3\text{C}_2\text{T}_x$ -SA. A scanning electronic microscope (SEM)

image of the $\text{Ti}_3\text{C}_2\text{T}_x$ particle showed a structure similar to that of an accordion in Fig. 2(a). The transmission electron microscope (TEM) analysis of the sample (Fig. 2(b)) depicts it to be quite thin and transparent to electrons. Fig. 2(c) illustrates the atomic lattice of $\text{Ti}_3\text{C}_2\text{T}_x$ -SA under a high-resolution TEM (HRTEM). The inset shows the selected area electron scattering (SAED) pattern confirming the hexagonal symmetry of the planes. Fig. 2(d) shows the side-view of the HRTEM displaying a bilayer structure of the as-exfoliated carbon layer. It can be seen from the figure that the layer thickness of $\text{Ti}_3\text{C}_2\text{T}_x$ is about 1 nm. In addition, we measured the nonlinear saturable absorption properties of $\text{Ti}_3\text{C}_2\text{T}_x$ by a mode-locked Tm-doped fiber laser with a 23.6 ps pulse duration and 31 MHz repetition rate at 2000 nm. The transmittance was detected by varying intensity of the laser seed source power. Fig. 3 shows the modulation depth of $\text{Ti}_3\text{C}_2\text{T}_x$ -SA was 26.6%.

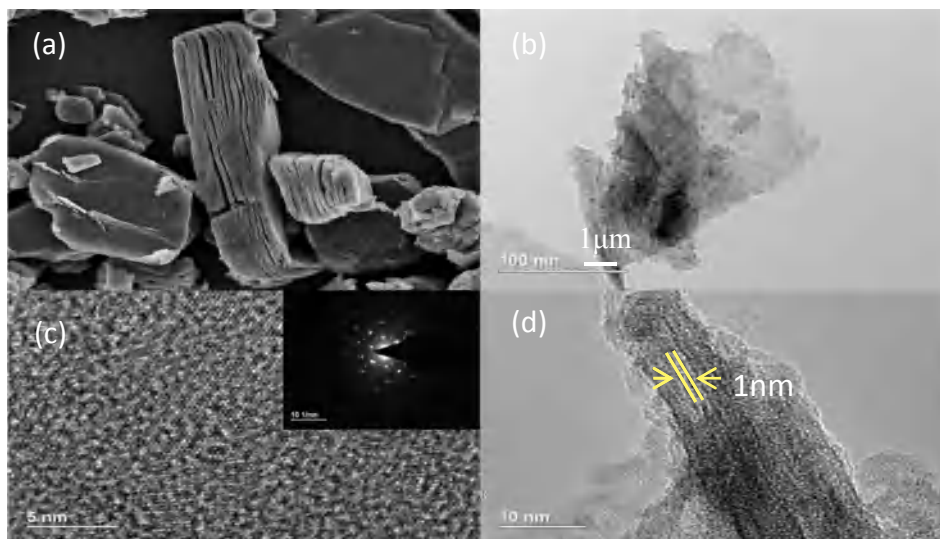


Fig. 2. (a) SEM images of the delaminated $\text{Ti}_3\text{C}_2\text{T}_x$. (b) TEM image characterizing the surface morphology of $\text{Ti}_3\text{C}_2\text{T}_x$. (c) HRTEM of $\text{Ti}_3\text{C}_2\text{T}_x$. Inset: SAED image. (d) Side-view of the HRTEM.

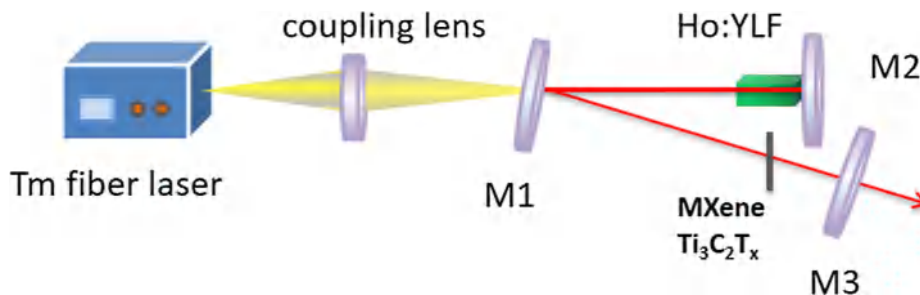


Fig. 4. Schematic of the experimental facility for the PQS operations.

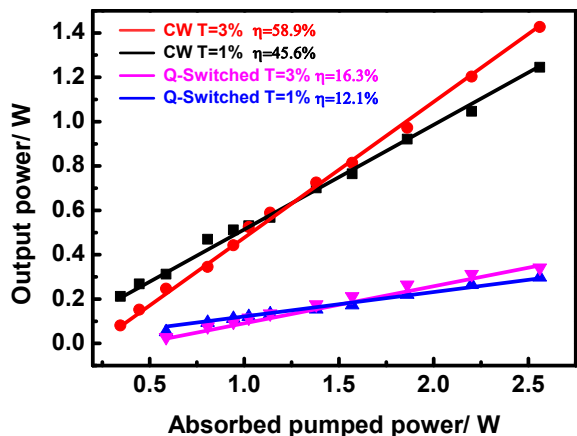


Fig. 5. Output power versus the absorbed pump powers for CW and PQS.

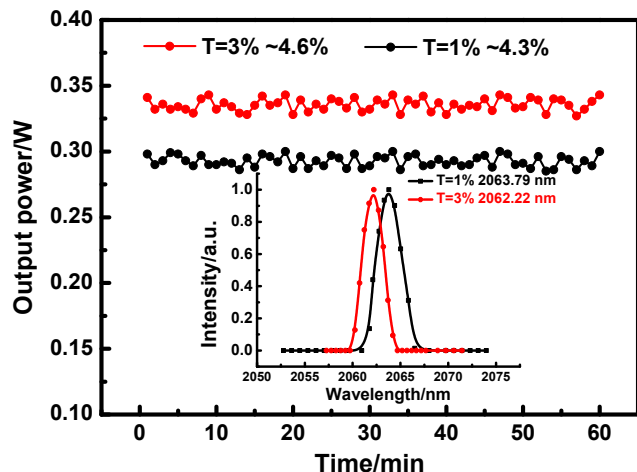


Fig. 6. Instability of the average output power measured during 60 min with OCs. Inset: PQS laser emission spectra for two different OCs.

3. Experimental setup

Fig. 4 schematically shows the experimental facility of the Ho: YLF pulse laser. A commercial Tm: fiber laser (TDFL01-00015), whose

wavelength was 1940 nm, was used as the pump source. A lens with 100 mm focal length was applied to collimate and focus the pump light into the laser media. The Ho: YLF (3 mm * 3 mm * 10 mm) crystal was placed into a Cu holder and stabilized at 13 °C. The crystal has dopant concentrations of 0.5% Ho and both end faces of the crystal are AR coated at 1940 nm and 2050 nm. The size of the pump spot radius in the Ho: YLF was gauged to be approximately 102 μm by the 90/10 knife edge method [38], which can well be suited with the oscillation spot. A V-shaped stabilized optical resonator comprised a flat mirror M1 ($T > 99\%$ at the wavelength of 1850–1950 nm and $R > 99\%$ at the wavelength of 2050–2150 nm), a flat high-reflective mirror M2, and a plano-concave output coupler (OC) M3 (radius of curvature: 200 mm) to prevent the return of the laser to break the Tm: fiber laser. Two OCs with different transmissions of 1% and 3% at 2050–2150 nm were tested. The length of the resonant cavity designed in the experiment is 178 mm.

4. Results and discussion

First, the continuous wave (CW) laser mode without $Ti_3C_2T_x$ -SA was performed when the absorbed pump power was 0.32 W. Fig. 5 displays the correlation between the output power and the absorbed pump power with two different OCs. The laser output power quite linearly increases with the absorbed pump power, and no noticeable saturation tendency was observed. The maximum average output power of 1.43 W with a slope efficiency of 58.9% was obtained. The laser threshold was 2.56 W by transmission of 3% OC.

$Ti_3C_2T_x$ -SA was then installed in the resonator with a 30 mm distance of OC. By using the calculated ABCD matrix, the radius of the TEM00 mode at the location $Ti_3C_2T_x$ -SA was found to be approximately 120 μm. The position and the angle were carefully adjusted such that the laser can operate in a PQS mode. When the absorbed pump power was 0.62 W, the stable pulse trains begin to appear. The maximum output power of 298 mW and 341 mW were obtained with $T = 1\%$ and $T = 3\%$ OC under the absorbed pump power of 2.56 W (Fig. 5). Fig. 6 describes that the stability of the two OC maximum output powers were approximately 4.3% and 4.6% in 60 min. The pulse laser emission spectra for the two different OCs were centered at 2063.8 nm and 2062.2 nm, respectively, and recorded by an optical spectrum instrument (SOL-MS3504i) with a wavelength resolution of 0.34 nm (inset, Fig. 6).

Fig. 7(a)–(d) show the pulse repetition rate, pulse width, single pulse energy, and peak power as functions of the absorbed pump power for different transmissions. The repetition frequency, single pulse energy, and peak power increased as the pump power increased in both experiments; however, the pulse width became narrower. When using

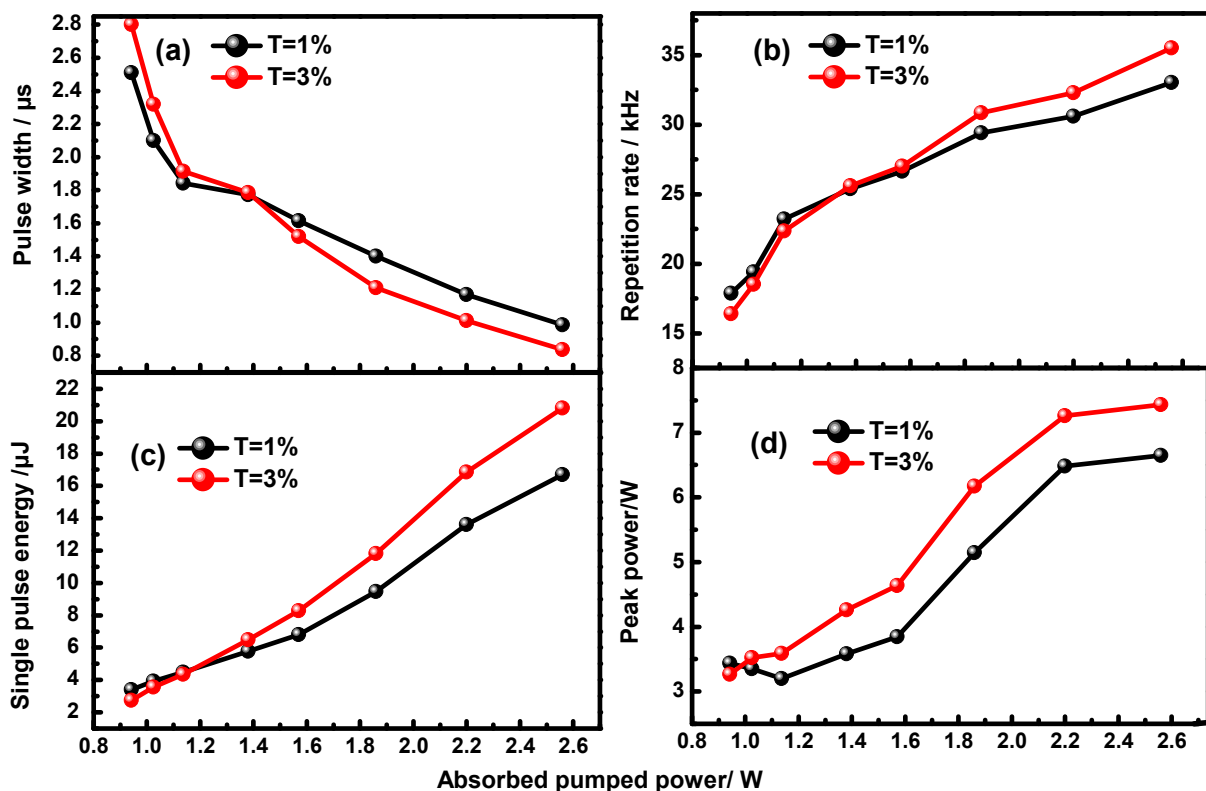


Fig. 7. (a) Pulse durations, (b) repetition rates, (c) single pulse energies, and (d) peak powers as functions of the absorbed pump powers.

Table 1

Performances of the PQS Ho:YLF laser under different OCs.

Transmittance of the OC	T = 1%	T = 3%
Shortest pulse width/ns	986	837
Repetition rate/kHz	33.03	35.5
Peak power/W	6.65	7.43
Single pulse energy/ μJ	16.69	20.8

T = 3% OC, the shortest pulse width was 837 ns, and the highest pulse repetition rate was 35.5 kHz, leading to a pulse energy of 20.8 μJ and a peak power of 7.43 W. Table 1 summarizes the detailed experimental conclusions.

Fig. 8 depicts the typical pulse trains at the maximum average output power captured by a 1 GHz digital oscilloscope (MDO4104C, Tektronix) and a fast photodiode detector (ET-5000, Electro-Optics). Finally, the M^2 values of the Q-switched Ho: YLF laser with T = 3% OC were measured with the 90/10 knife-edge way in Fig. 9 and estimated as 1.5 and 1.6 for the horizontal and vertical directions, respectively. We employed the NS2-Pyro/9/5-PRO (Photon) apparatus to record the

laser beam profile and the three-dimensional light intensity map, as displayed in insets (a) and (b) of Fig. 9.

5. Conclusions

In conclusion, $\text{Ti}_3\text{C}_2\text{T}_x$ MXene was successfully prepared herein by the acid etching process and as SA employed in an in-band pumped Ho pulse laser at 2.1 μm . The shortest pulse width of the Q-switched laser was 837 ns. The maximum single pulse energy was 20.8 μJ at a repetition rate of 35.5 kHz. To the best of our knowledge, this is the first report presenting a $\text{Ti}_3\text{C}_2\text{T}_x$ -based PQS Ho: YLF laser by a Tm-doped fiber laser pump. The results suggest the promising potential of $\text{Ti}_3\text{C}_2\text{T}_x$ as an efficient optical modulator for short-pulse lasers.

Declaration of Competing Interest

This manuscript has not been published or presented elsewhere in part or in entirety and is not under consideration by another journal. We have read and understood your journal's policies, and we believe that neither the manuscript nor the study violates any of these. There are no conflicts of interest to declare.

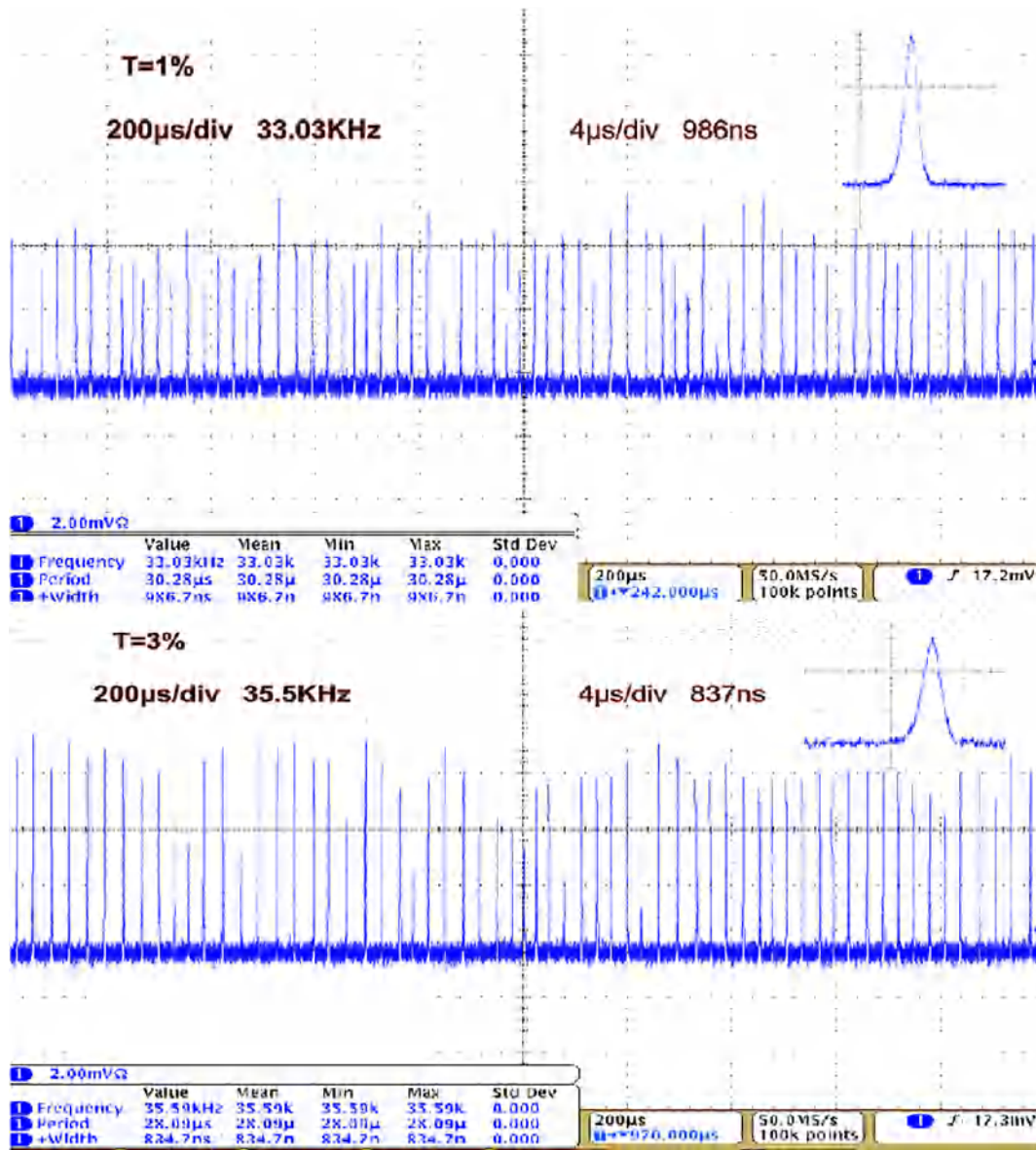


Fig. 8. Oscilloscope display of PQS pulse trains at the maximum output power.

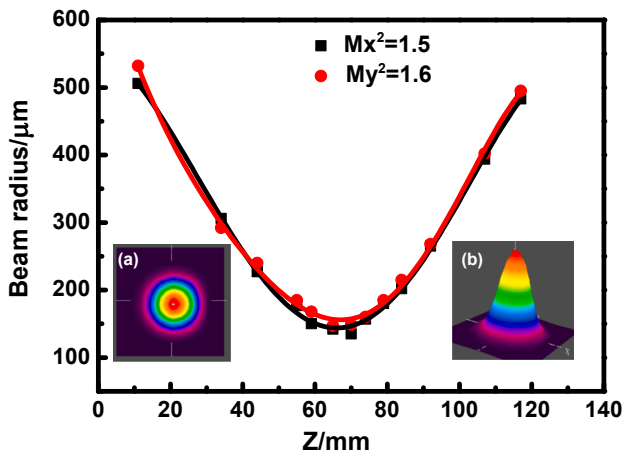


Fig. 9. Beam quality and spatial beam profile.

Acknowledgements

This work was supported in part by the the National Natural Science Foundation of China (NSFC) (11974220,61435010), and Science and Technology Planning Project of Guangdong Province (2016B050501005)

References

- [1] C.D. Nabors, J. Ochoa, T.Y. Fan, A. Sanchez, H.K. Choi, G.W. Turner, Ho:YAG laser pumped by 1.9- μm diode lasers, *IEEE J. Quantum Electron.* 31 (9) (1995) 1603–1605.
- [2] B.Q. Yao, X.M. Duan, L.L. Zheng, Y.L. Ju, Y.Z. Wang, G.J. Zhao, Q. Dong, Continuous-wave and Q-switched operation of a resonantly pumped Ho:YAlO₃ laser, *Opt. Express* 16 (19) (2008) 14668–14674.
- [3] X.T. Yang, Y.B. He, X.N. Liu, Z.Y. Jiang, S.T. Chen, Y.L. Mu, L.L. Yang, Z.J. Zhang, N.B. Zhao, A passively Q-switched Ho:SSO laser with a Cr²⁺: ZnSe saturable absorber, *Infrared Phys. Technol.* 98 (2019) 121–124.
- [4] X.M. Duan, Y.J. Shen, J. Gao, H.B. Zhu, C.P. Qian, L.B. Su, L.H. Zheng, L.J. Li, B.Q. Yao, T.Y. Dai, Active Q-switching operation of slab Ho:SYSO laser wing-pumped by fiber coupled laser diodes, *Opt. Express* 27 (8) (2019) 11455–11461.

- [5] K. Scholle, S. Lamrini, P. Koopmann, P. Fuhrberg, 2 μm laser sources and their possible applications, *Frontiers in Guided Wave Optics and Optoelectronics*, Intech Open, 2010.
- [6] E.C. Ji, Q. Liu, M.M. Nie, X.Z. Cao, X. Fu, M.L. Gong, High-slope-efficiency 2.06 μm Ho:YLF laser in-band pumped by a fiber-coupled broadband diode, *Opt. Lett.* 41 (6) (2016) 1237–1240.
- [7] B.M. Walsh, N.P. Barnes, B.D. Bartolo, Branching ratios, cross sections, and radiative lifetimes of rare earth ions in solids: application to Tm^{3+} and Ho^{3+} ions in LiYF_4 , *J. Appl. Phys.* 83 (5) (1998) 2772–2787.
- [8] C. Yang, Y.L. Ju, B.Q. Yao, T.Y. Dai, X.M. Duan, J. Li, Y. Ding, W. Liu, Y.B. Pan, C.Y. Li, Passively Q-switched Ho:YLF laser pumped by Tm^{3+} -doped fiber laser, *Opt. Laser Technol.* 77 (2016) 55–58.
- [9] B.Q. Yao, X.L. Li, Z. Cui, T.Y. Dai, S. Bai, H.Y. Yang, X.M. Duan, Y.L. Ju, High-repetition rate passively Q-switched Ho:YLF laser with graphene as a saturable absorber, *Opt. Eng.* 54 (7) (2015) 76105.
- [10] Z. Cui, B.Q. Yao, X.M. Duan, J. Li, S. Bai, X.L. Li, Y. Zhang, J.H. Yuan, T.Y. Dai, Y.L. Ju, C.Y. Li, Y.B. Pan, Experimental study on a passively Q-switched Ho:YLF laser with polycrystalline $\text{Cr}^{2+}:\text{ZnS}$ as a saturable absorber, *Chin. Phys. Lett.* 32 (08) (2015) 84205–084205.
- [11] Z.Q. Li, Y.X. Zhang, C. Cheng, H. Yu, F. Chen, 6.5 GHz Q-switched mode-locked waveguide lasers based on two-dimensional materials as saturable absorbers, *Opt. Express* 26 (2018) 11321–11330.
- [12] J.J. Liu, H. Huang, F. Zhang, Z. Zhang, J. Liu, H. Zhang, L.B. Su, Bismuth nanosheets as a Q-switcher for a mid-infrared erbium-doped SrF_2 laser, *Photonics Res.* 6 (2018) 762–767.
- [13] C. Zhang, J. Liu, X.W. Fan, Q.Q. Peng, X.S. Guo, D.P. Jiang, X.B. Qian, L.B. Su, Compact passive Q-switching of a diode-pumped Tm, Y:CaF₂ laser near 2 μm , *Opt. Laser Technol.* 103 (2018) 89–92.
- [14] P.G. Ge, J. Liu, S.Z. Jiang, Y.Y. Xu, B.Y. Man, Compact Q-switched 2 μm Tm:GdVO₄ laser with MoS₂ absorber, *Photonics Res.* 3 (5) (2015) 256–259.
- [15] Y.F. Ma, B.F. Ran, Z.F. Peng, S.J. Ding, H.Y. Sun, Q.L. Zhang, Diode-pumped two-dimensional MoS₂ passively Q-switched Nd:GdYNbO₄ laser, *Infrared Phys. Technol.* 98 (2019) 311–314.
- [16] Z.Q. Li, R. Li, C. Pang, N.N. Dong, J. Wang, H.H. Yu, F. Chen, 8.8 GHz Q-switched mode-locked waveguide lasers modulated by PtSe₂ saturable absorber, *Opt. Express* 27 (2019) 8727–8737.
- [17] J.J. Liu, X.Y. Feng, X.W. Fan, Z. Zhang, B. Zhang, J. Liu, L.B. Su, Efficient continuous-wave and passive Q-switched mode-locked $\text{Er}^{3+}:\text{CaF}_2\text{-SrF}_2$ lasers in the mid-infrared region, *Opt. Lett.* 43 (10) (2018) 2418–2421.
- [18] Z.Z. Chu, J. Liu, Z.N. Guo, Han Zhang, 2 μm passively Q-switched laser based on black phosphorus, *Opt. Mater. Exp.* 6 (7) (2016) 2374–2379.
- [19] X.Y. Feng, B.Y. Ding, W.Y. Liang, F. Zhang, T.Y. Ning, J. Liu, H. Zhang, MXene $\text{Ti}_3\text{C}_2\text{T}_x$ absorber for a 1.06 μm passively Q-switched ceramic laser, *Laser Phys. Lett.* 15 (2018) 085805.
- [20] C. Wang, Q.Q. Peng, X.W. Fan, W.Y. Liang, F. Zhang, J. Liu, H. Zhang, MXene $\text{Ti}_3\text{C}_2\text{T}_x$ saturable absorber for pulsed laser at 1.3 μm , *Chin. Phys. B* 27 (2018) 094214.
- [21] Y.Q. Zu, C. Zhang, X.S. Guo, W.Y. Liang, J. Liu, L.B. Su, H. Zhang, A solid-state passively Q-switched Tm, Gd:CaF₂ laser with a $\text{Ti}_3\text{C}_2\text{T}_x$ MXene absorber near 2 μm , *Laser Phys. Lett.* 16 (2019) 15803.
- [22] Q. Yang, F. Zhang, N.Y. Zhang, H. Zhang, Few-layer MXene $\text{Ti}_3\text{C}_2\text{T}_x$ (T = F, O, or OH) saturable absorber for visible bulk laser, *Opt. Mater. Exp.* 9 (2019) 1795–1802.
- [23] X.L. Sun, B.T. Zhang, B.Z. Yan, G.R. Li, H.K. Nie, K.J. Yang, C.Q. Zhang, J.L. He, Few-layer $\text{Ti}_3\text{C}_2\text{T}_x$ (T = O, OH, or F) saturable absorber for a femtosecond bulk laser, *Opt. Lett.* 43 (2018) 3862–3865.
- [24] K. Rasool, M. Helal, A. Ali, C.E. Ren, Y. Gogotsi, K.A. Mahmoud, Antibacterial Activity of $\text{Ti}_3\text{C}_2\text{T}_x$ MXene, *ACS Nano* 10 (3) (2016) 3674–3684.
- [25] K. Hantanasirisakul, M.Q. Zhao, P. Urbankowski, J. Halim, B. Anasori, S. Kota, C.E. Ren, M.W. Barsoum, Y. Gogotsi, Fabrication of $\text{Ti}_3\text{C}_2\text{T}_x$ MXene transparent thin films with tunable optoelectronic properties, *Adv. Electron. Mater.* 2 (6) (2016) 1600050.
- [26] C. Wang, Y.Z. Wang, X.T. Jiang, J.W. Xu, W.C. Huang, F. Zhang, J.F. Liu, F.M. Yang, Y.F. Song, Y.Q. Ge, Q. Wu, M. Zhang, H. Chen, J. Liu, H. Zhang, MXene $\text{Ti}_3\text{C}_2\text{T}_x$: A promising photothermal conversion material and application in All-optical modulation and All-optical information loading, *Adv. Opt. Mater.* 1900060 (2019).
- [27] A. Miranda, J. Halim, M.W. Barsoum, A. Lorke, Electronic properties of free-standing $\text{Ti}_3\text{C}_2\text{T}_x$ MXene monolayers, *Appl. Phys. Lett.* 108 (3) (2016) 033102.
- [28] X.Q. Fan, L. Liu, X. Jin, W.T. Wang, S.F. Zhang, B.T. Tang, MXene $\text{Ti}_3\text{C}_2\text{T}_x$ for phase change composite with superior photothermal storage capability, *J. Mater. Chem. A* 10 (2019) 1039.
- [29] M. Naguib, V. Mochalin, M. Barsoum, Y. Gogotsi, 25th anniversary article: MXenes: a new family of two-dimensional materials, *Adv. Mater.* 26 (7) (2014) 992–1005.
- [30] X. Jiang, S. Liu, W. Liang, S. Luo, Z. He, Y. Ge, H. Wang, R. Cao, F. Zhang, Q. Wen, J. Li, Q. Bao, D. Fan, H. Zhang, Broadband nonlinear photonics in few-layer MXene $\text{Ti}_3\text{C}_2\text{T}_x$ (T = F, O, or OH), *Laser Photonics Rev.* 12 (2) (2018) 1700229.
- [31] J. Liu, H.B. Zhang, R.H. Sun, Y.F. Liu, Z.S. Liu, A.G. Zhou, Z.Z. Yu, Hydrophobic, flexible, and lightweight MXene foams for high-performance electromagnetic-interference shielding, *Adv. Mater.* 29 (38) (2017) 1702367.
- [32] C.Y. Shi, M. Beidaghi, M. Naguib, O. Mashtalir, Y. Gogotsi, S.J.L. Billinge, Structure of Nanocrystalline Ti_3C_2 MXene using atomic pair distribution function, *Phys. Rev. Lett.* 112 (12) (2014) 125501.
- [33] R.R. Nair, P. Blake, A.N. Grigorenko, K.S. Novoselov, T.J. Booth, T. Stauber, N.M.R. Peres, A.K. Geim, Fine structure constant defines visual transparency of graphene, *Science* 320 (5881) (2008) 1308–1308.
- [34] Q. Wu, X. Jin, S. Chen, X. Jiang, Y. Hu, Q. Jiang, L. Wu, J. Li, Z. Zheng, M. Zhang, H. Zhang, MXene-based saturable absorber for femtosecond mode-locked fiber lasers, *Opt. Express* 27 (2019) 10159–10170.
- [35] Y.C. Dong, S. Chertopalov, K. Maleski, B. Anasori, L.Y. Hu, S. Bhattacharya, A.M. Rao, Y. Gogotsi, V.N. Mochalin, R. Podila, Saturable absorption in 2D Ti_3C_2 MXene thin films for passive photonic diodes, *Adv. Mater.* 30 (10) (2018) 1705714.
- [36] Y. Zhang, Y. Huang, T.F. Zhang, H.C. Chang, P.S. Xiao, H.H. Chen, Z.Y. Huang, Y.S. Chen, Broadband and tunable high-performance microwave absorption of an ultralight and highly compressible graphene foam, *Adv. Mater.* 27 (12) (2015) 2049–2053.
- [37] Y.J. Zhang, W.Y. Xia, Y.B. Wu, Peihong Zhang, Prediction of MXene based 2D tunable band gap semiconductors: GW quasiparticle calculations, *Nanoscale* 11 (9) (2019) 3993–4000.
- [38] Q. Dong, G.J. Zhao, D.H. Cao, B.Q. Yao, X.T. Yang, Z.P. Yu, Polarized spectral analysis of Ho^{3+} ions in biaxial YAlO_3 crystal for 2 μm lasers, *J. Phys. D Appl. Phys.* 42 (4) (2009) 045114.